

Ruthenium xantphos complexes in hydrogen transfer processes: reactivity and mechanistic studies†

Araminta E. W. Ledger, Paul A. Slafford, John P. Lowe, Mary F. Mahon, Michael K. Whittlesey* and Jonathan M. J. Williams*

Received 5th August 2008, Accepted 17th September 2008

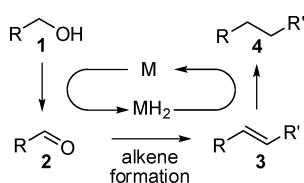
First published as an Advance Article on the web 27th November 2008

DOI: 10.1039/b813543f

The *in situ* combination of $[\text{Ru}(\text{PPh}_3)_3(\text{CO})\text{H}_2]$ with xantphos is catalytically active for the alkylation of alcohols with the ketonitrile $t\text{BuC}(\text{O})\text{CH}_2\text{CN}$ in a model oxidation–Knoevenagel–reduction process. The precursor complex $[\text{Ru}(\text{xantphos})(\text{PPh}_3)(\text{CO})\text{H}_2]$ was isolated and reacted with stoichiometric amounts of PhCH_2OH and PhCHO . Under these conditions, the alcohol is decarbonylated to afford $[\text{Ru}(\text{xantphos})(\text{CO})_2\text{H}_2]$ and finally $[\text{Ru}(\text{xantphos})(\text{CO})_3]$, both of which prove to be less active for catalysis than the starting complex. The reactivity of the xantphos system contrasts with that of $[\text{Ru}(\text{dppp})(\text{PPh}_3)(\text{CO})\text{H}_2]$, which is catalytically inactive for the Knoevenagel reaction and fails to show any stoichiometric reactivity with alcohols.

Introduction

Ruthenium complexes have been widely used as catalysts for hydrogen transfer reactions, especially in the reduction of ketones to secondary alcohols.¹ The metal-catalysed transfer of hydrogen from alcohols to alkenes has been of significant importance in the formation of new C–C bonds by the borrowing hydrogen strategy outlined in Scheme 1. A transition metal catalyst temporarily removes hydrogen from an alcohol **1** to generate the more electrophilic aldehyde **2**. This intermediate aldehyde undergoes *in situ* transformation into an alkene **3**, which is then reduced to generate the new C–C bond in product **4** by return of the hydrogen from the catalyst. The borrowing hydrogen strategy avoids the requirement for traditional alkylating agents, such as alkyl halides.

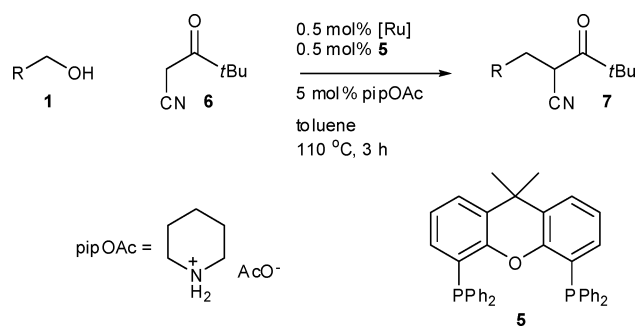


Scheme 1 Borrowing hydrogen in the formation of C–C bonds from alcohols.

The first examples of homogeneous catalysts for such chemistry were reported by Grigg *et al.* in 1981.² There have been many other catalysts reported since,³ especially ruthenium,⁴ iridium⁵ and palladium⁶ based systems. We have previously reported the use of an iridium complex⁷ and an *N*-heterocyclic carbene ruthenium

complex⁸ for the formation of C–C bonds from alcohols by indirect Wittig reactions, which proceed *via* the aldehyde and alkene.

Recently, we reported that the combination of $[\text{Ru}(\text{PPh}_3)_3(\text{CO})\text{H}_2]$ with bidentate phosphines can afford an effective catalyst for the alkylation of the ketonitrile **6** with alcohols (Scheme 2). Particularly striking was the high activity found when the added ligand was xantphos **5**.⁹ The $[\text{Ru}(\text{PPh}_3)_3(\text{CO})\text{H}_2]$ /xantphos combination has subsequently proved to be highly effective for other processes including the conversion of alkynediols into furans¹⁰ and pyrroles,¹¹ as well as the elimination of alcohols from oxime ethers to give nitriles.¹²



Scheme 2 Catalytic C–C bond formation with $[\text{Ru}(\text{PPh}_3)_3(\text{CO})\text{H}_2]$ and xantphos.

In light of the high activity of the *in situ* generated ruthenium xantphos system, we have now prepared and isolated the precursor complex $[\text{Ru}(\text{xantphos})(\text{PPh}_3)(\text{CO})\text{H}_2]$ (**18**) and studied its stoichiometric reactivity towards alcohols and aldehydes. The reactivity of **18** is contrasted with $[\text{Ru}(\text{dppp})(\text{PPh}_3)(\text{CO})\text{H}_2]$ (**19**, $\text{dppp} = \text{Ph}_2\text{P}(\text{CH}_2)_3\text{PPh}_2$), which proves to be ineffective for the catalytic reaction in Scheme 2. We now show that whereas **18** oxidises benzyl alcohol, **19** is totally inert. Moreover, under stoichiometric conditions, decarbonylation of benzyl alcohol by **18** also takes place to afford $\text{Ru}(\text{II})$ and $\text{Ru}(\text{0})$ species that prove to be less catalytically active than the starting material. These results

Department of Chemistry, University of Bath, Claverton Down, Bath, UK BA2 7AY. E-mail: chsmkw@bath.ac.uk, chsjmjw@bath.ac.uk; Fax: +44 1225 386 231; Tel: +44 1225 383 942

† Electronic supplementary information (ESI) available: spectroscopic data for compounds **7b–k** are provided, along with crystallographic data for complex **22**. CCDC reference numbers 678477 (**18**), 678478 (**20**) and 678479 (**22**). For ESI and crystallographic data in CIF or other electronic format see DOI: 10.1039/b813543f

Table 1 Activity of [Ru(PPh₃)₃(CO)H₂]-phosphine combinations for reaction of **1** with **6**^a

Ligand ^b	Catalyst loading/mol%	Time/h	Conversion (%)
None	5	18	56
Dppe	5	1	4
Dppp	5	1	<1
Dppf 9	5	1	74
Dppf 9	0.5	3	56
10	0.5	3	91
Xantphos 5	0.5	3	100
11	0.5	3	0
DPEphos 8	0.5	3	8

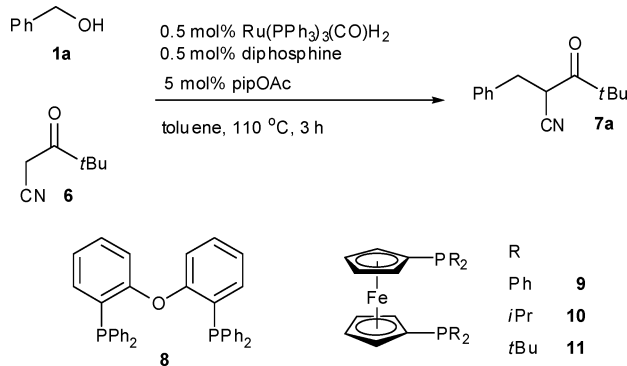
^a Reaction conditions: benzyl alcohol (**1a**) 1 equiv., ketonitrile (**6**) 1 equiv., piperidinium acetate 5 mol%, toluene, 120 °C, 3 h. ^b A 1 : 1 ratio of [Ru(PPh₃)₃(CO)H₂] to ligand was used in all cases.

suggest that the success of **18** in catalysing the reaction shown in Scheme 2 is not only due to the ability of the catalyst precursor to react with the alcohol in the first place, but also because of the fact that **6** is able to react with the intermediate aldehyde before it is decarbonylated by ruthenium to form less active metal based species.

Results and discussion

Catalytic Activity of [Ru(PPh₃)₃(CO)H₂]-phosphine

As we have previously reported, the alkylation of ketonitrile **6** with benzyl alcohol **1a** (Scheme 3) was catalysed by an *in situ* mixture of [Ru(PPh₃)₃(CO)H₂] and a range of bidentate phosphorus ligands as shown in Table 1. The parent complex [Ru(PPh₃)₃(CO)H₂] showed some catalytic activity in the absence of any added ligands (although over quite a long reaction time), however, the addition of one equivalent of either of the ferrocene based ligands **9** or **10**,¹³ or xantphos **5**,¹⁴ provided a much more reactive system that gave good conversions to **7a** at only 0.5 mol% catalyst loading. The subtle nature of the stereoelectronic effects at play in the catalysis was well illustrated by the fact that the bulky ferrocene derivative **11** as well as the flexible P,O,P ligand DPEphos **8**¹⁵ proved to be completely inactive. Of equal note was the failure of the more common chelating phosphines dppe and dppp to give any product formation.

**Scheme 3** Ligand screening in the benzylation of ketonitrile **6**.

Subsequent studies showed that the [Ru(PPh₃)₃(CO)H₂]-xantphos combination could be applied to the coupling of **6** with

Table 2 Range of alcohols examined in the alkylation of ketonitrile **6** with [Ru(PPh₃)₃(CO)H₂]-xantphos^a

R	Catalyst loading (mol%) ^b	Conversion (%)	Yield (%)
Ph (1a)	0.5	100	78
<i>p</i> -MeOC ₆ H ₄ (1b)	0.5	100	83
<i>o</i> -MeOC ₆ H ₄ (1c)	0.5	100	82
<i>p</i> -FC ₆ H ₄ (1d)	0.5	100	89
<i>p</i> -BrC ₆ H ₄ (1e)	0.5	100	79
<i>p</i> -O ₂ NC ₆ H ₄ (1f)	0.5	52	31
<i>p</i> -F ₃ CC ₆ H ₄ (1g)	0.5	100	83
Furyl (1h)	5	100	72
PhCH ₂ (1i)	2.5	100	87
C ₁₀ H ₂₁ (1j)	5	100	85
Cyclopropyl (1k)	5	100	69
IndenylCH ₂ (1l)	5	100	76

^a Reaction conditions: alcohol 1 equiv., ketonitrile (**6**) 1 equiv., piperidinium acetate 5 mol%, toluene, reflux, 4 h. ^b A 1 : 1 ratio of [Ru(PPh₃)₃(CO)H₂] to xantphos was used in all cases.

a range of alcohols. With benzylic alcohols (**1a–e**, **g**, Table 2), a catalyst loading of 0.5 mol% was sufficient to achieve 100% conversion in 3 h with correspondingly good isolated yields with the exception of the *p*-nitro-substituted benzyl alcohol (**1f**) and furfuryl alcohol (**1h**), although in the latter case, complete conversion was obtained with a higher catalyst loading. As complete conversions were seen in many cases after 3 h, the reactions with **1a**, **1b** and **1d** were run for shorter times (1.5 h, not shown in Table 2) to establish whether there was an electronic influence on reaction rate. The results for benzyl alcohol **1a** (88%), *p*-methoxybenzyl alcohol **1b** (95%) and *p*-fluorobenzyl alcohol **1d** (70%) suggest that the relative ease of oxidation of the alcohols to the intermediate aldehydes is a limiting factor in the overall process. Further support for this argument was provided by the lower reactivity associated with the aliphatic alcohols **1i–l**.

The success of xantphos prompted us to investigate other xanthene based ligands **12–17** (Fig. 1) for the reaction shown in Scheme 3. Two of the ligands, sixantphos **13** and isopropylxantphos **15** were found to give a somewhat improved reactivity compared to the parent xantphos (Table 3), although the commercial availability of **5** was the reason that it was used for all subsequent studies of stoichiometric reactivity. One conclusion clearly supported by the data in Table 3 is that in contrast to other catalysis employing xanthene based ligands, there is no obvious correlation between the reactivity and the reported natural bite angles of the ligands.¹⁶

Table 3 Activity of added xanthene ligands for the reaction in Scheme 3^a

Ligand ^b	Bite angle/° ^c	Conversion (%)
Homoxantphos 12	102.0	46
Sixantphos 13	108.5	98
Thixantphos 14	109.6	77
Xantphos 5	111.4	81
Isopropylxantphos 15	113.2	92
Nixantphos 16	114.2	3
Benzylnixantphos 17	114.1	4

^a Reaction conditions: alcohol 1 equiv., ketonitrile (**6**) 1 equiv., [Ru(PPh₃)₃(CO)H₂] 0.5 mol%, piperidinium acetate 5 mol%, toluene, 110 °C, 3.5 h. ^b A 1 : 1 ratio of [Ru(PPh₃)₃(CO)H₂] to xanthene ligand was used in all cases. ^c See ref. 17.

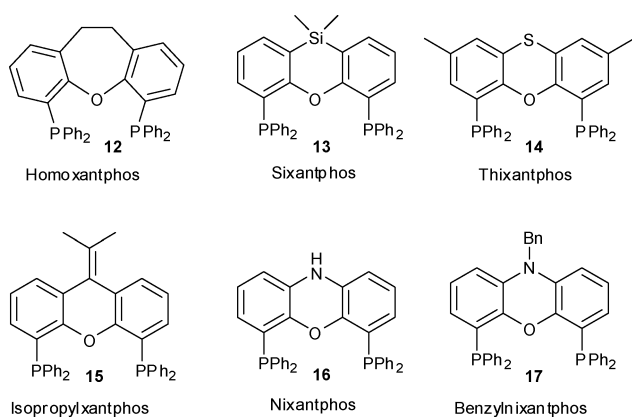


Fig. 1 Xanthene ligands tested in the benzylation of ketonitrile 6.

Synthesis and characterisation of $[\text{Ru}(\text{PPh}_3)_3(\text{CO})\text{H}_2]$ -phosphine precursors

In order to understand the activity associated with $[\text{Ru}(\text{PPh}_3)_3(\text{CO})\text{H}_2]$ and xantphos, and conversely the low activity found upon using dppp, both of the precursor complexes $[\text{Ru}(\text{xantphos})(\text{PPh}_3)(\text{CO})\text{H}_2]$ **18** and $[\text{Ru}(\text{dppp})(\text{PPh}_3)(\text{CO})\text{H}_2]$ **19**¹⁸ were prepared and isolated. In contrast to the sharp room temperature $^{31}\text{P}\{^1\text{H}\}$ NMR spectrum seen for **19**, **18** displayed two broad resonances for the xantphos ligand at δ 45.2 and 30.5 ppm and a sharp doublet of doublets at δ 58.5 ppm [$J_{\text{PP}} = 237.1$ Hz, 15.5 Hz] for the PPh_3 group.¹⁹ Upon cooling to 199 K, the signal at δ 45.2 ppm resolved into a doublet of doublets with J_{PP} values of 237.1 and 15.5 Hz, the larger splitting arising from coupling to the *trans* PPh_3 ligand. The two hydride resonances in the proton spectrum were also somewhat broad at 298 K (Fig. 2), and although they sharpened to some extent upon cooling to 199 K, this was not enough to resolve J_{HP} and J_{HH} values accurately. The coupling constants were determined from the simulated spectrum, which is shown with the experimental data in Fig. 2. While we were unable to elucidate the exact reason for the broadening of the resonances of **18**,²⁰ there are a number of reports that support the flexibility of xantphos.²¹

The molecular structure of **18** was determined by X-ray crystallography as shown in Fig. 3. The chelating xantphos ligand coordinates to the ruthenium centre in axial and equatorial positions, with the PPh_3 ligand occupying the second axial position. As expected on the basis of the different bite angles

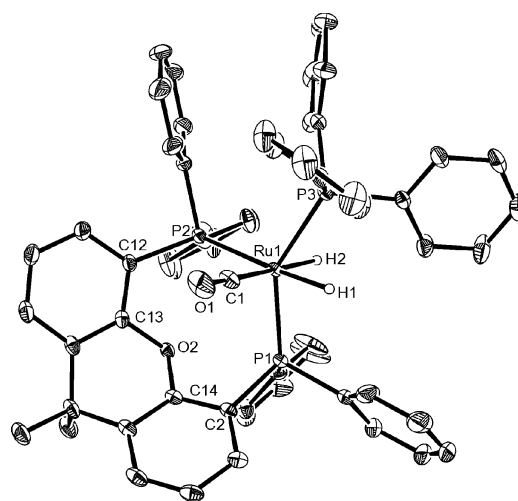
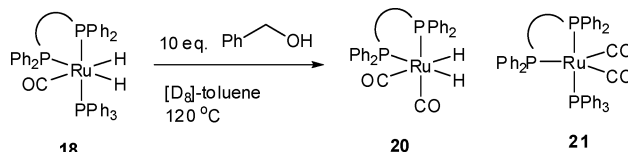


Fig. 3 Molecular structure of **18**.²³ All hydrogen atoms except Ru–H are omitted. Thermal ellipsoids are shown at the 30% probability level. Selected bond lengths (Å) and angles ($^\circ$): Ru–P(1) 2.3283(6); Ru–P(2) 2.3950(6); Ru–P(3) 2.2973(6); Ru–C(1) 1.897(3); P(1)–Ru–P(2) 102.76(2); P(1)–Ru–P(3) 145.06(2); P(2)–Ru–P(3) 107.16(2).

of xantphos and dppp, the xantphos ligand enforces a wide P(1)–Ru–P(2) angle [$102.76(2)^\circ$] at ruthenium, distorting the octahedral geometry to a greater extent than in **19** [P(1)–Ru–P(2), $92.14(9)^\circ$].^{18b} This distortion is further manifested in the *trans*-P–Ru–P angles $145.06(2)$ and $160.67(9)^\circ$ for **18** and **19**, respectively.

Stoichiometric reactivity of benzyl alcohol with **18** and **19**

Quite different behaviour was observed upon heating **18** and **19** in the presence of 10 equivalents of PhCH_2OH in toluene at 120°C for 2 h. While in the case of **19**, ^1H NMR spectroscopy showed only unreacted starting material, the xantphos complex **18** was converted into a *ca.* 2 : 1 mixture of $[\text{Ru}(\text{xantphos})(\text{CO})_2\text{H}_2]$ **20** and



Scheme 4 Reactivity of $[\text{Ru}(\text{xantphos})(\text{PPh}_3)(\text{CO})\text{H}_2]$ (**18**) with benzyl alcohol.

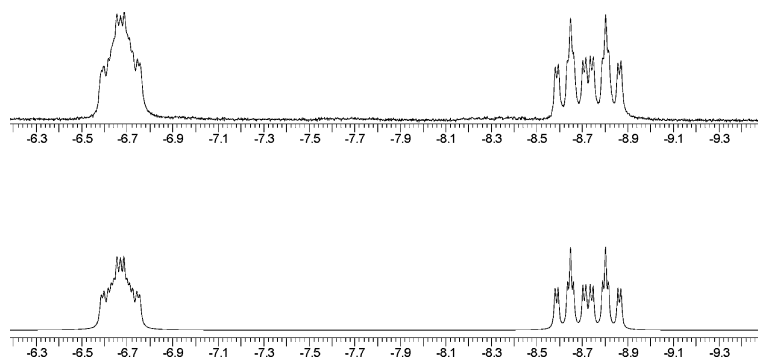


Fig. 2 Simulated²² (lower) and experimental (upper) ^1H NMR spectrum of **18** ($[\text{d}_8]$ -toluene, 500 MHz, 298 K). Calculated chemical shifts (ppm) and coupling constants (J): δ -6.67 ($J_{\text{HP}} = 35.0$, $J_{\text{HP}} = 28.0$, $J_{\text{HP}} = 15.5$, $J_{\text{HH}} = 6.6$ Hz), δ -8.72 ($J_{\text{HP}} = 77.0$, $J_{\text{HP}} = 33.9$ Hz, $J_{\text{HP}} = 27.3$, $J_{\text{HH}} = 6.6$ Hz).

[Ru(xantphos)(PPh₃)(CO)₂] **21** (Scheme 4).²⁴ PhCHO, benzene and H₂ were also detected. The dicarbonyl dihydride complex **20** displayed two doublet of doublet of doublet hydride resonances at δ -6.13 and -7.65 ppm; the large J_{HP} coupling constant of 82 Hz observed on the lower frequency signal showed it to be the one *trans* to phosphorus.²⁵ In the IR spectrum, two CO bands of equal intensity were found at 2007 and 1960 cm⁻¹, consistent with a *cis* arrangement of the carbonyl ligands observed for other reported [Ru(P-P)(CO)₂H₂] complexes.²⁶ The molecular structure of **20** was elucidated following an independent synthesis, which involved the photolysis of [Ru(xantphos)(CO)₃] **22**²⁷ under a purge of hydrogen at 0 °C. The X-ray structure of **20** (Fig. 4) showed a lengthening of the Ru-xantphos and Ru-CO distances compared to those found in **18** [Ru-CO, 1.958(5) Å; **18**: Ru-P 2.3283(6); Ru-P 2.3950(6) Å; Ru-CO 1.897(3) Å] and a widening of the *trans*-P-Ru-L angle from 145.06(2)° for L = PPh₃ in **18** to 156.18(10)° for L = CO in **20**.

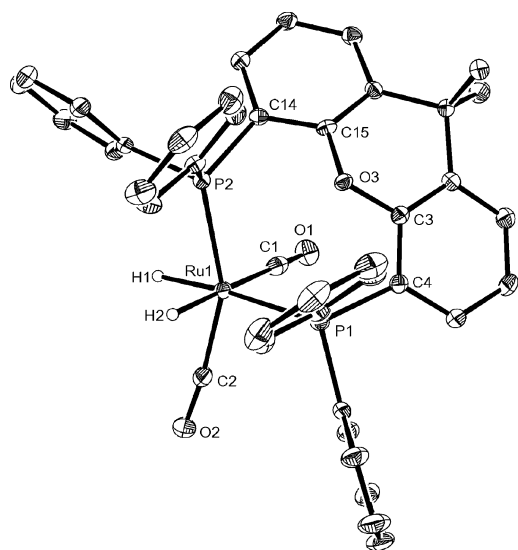


Fig. 4 Molecular structure of **20**.²⁹ All hydrogen atoms (except Ru-H) are omitted. Thermal ellipsoids are shown at the 30% probability level. Selected bond lengths (Å) and angles (°): Ru-P(1) 2.4146(8); Ru-P(2) 2.3805(9); Ru-C(1) 1.958(5); Ru-C(2) 1.878(4); P(1)-Ru-P(2) 102.20(3); P(1)-Ru-C(1) 91.89(10); P(1)-Ru-C(2) 92.86(10); P(2)-Ru-C(1) 95.98(10); P(2)-Ru-C(2) 156.18(10); C(1)-Ru-C(2) 101.92(15).

While the formation of benzaldehyde from PhCH₂OH is consistent with the ability of **18** to catalyse the Knoevenagel reaction in Scheme 2, the formation of **20**, benzene and H₂ shows that the ruthenium complex can also bring about the decarbonylation of alcohols under non-catalytic conditions. Indeed, when **18** was heated with Ph¹³CH₂OH, both [Ru(xantphos)(¹³CO)(CO)H₂] and [Ru(xantphos)(¹³CO)₂H₂] were formed (some ¹³CO labelled **18** and Ph¹³CHO was also detected). Complex **20** was also capable of decarbonylation chemistry; reaction of the complex with 5 equivalents of PhCH₂OH gave the tricarbonyl species **22** as the final ruthenium containing product of the reaction. While further studies showed that **18** would decarbonylate a range of aromatic alcohols, including Ph(CH₂)_nOH (*n* = 1, 2, 3) and 1,2-C₆H₄(CH₂OH)₂, efforts to make the process catalytic were prevented by ease with which **22** was formed and its lack of reactivity towards either alcohols or aldehydes. Attempts to inhibit

Table 4 Catalytic activity of xantphos complexes **20–22** for reaction of **1a** with **6**^a

Catalyst ^b	Loading (mol%)	Time/h	Conversion (%)
[Ru(xantphos)(CO) ₂ H ₂] 20	0.5	0.5	55
[Ru(xantphos)(PPh ₃)(CO) ₂] 21	0.5	0.5	4
[Ru(xantphos)(CO) ₃] 22	0.5	0.5	30

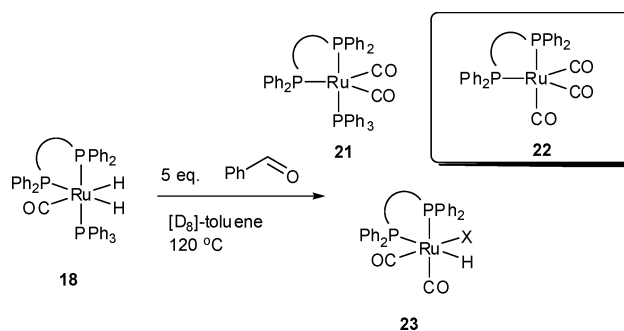
^a Reaction conditions: alcohol 1 equiv., ketonitrile (**6**) 1 equiv., piperidinium acetate 5 mol%, refluxing toluene, 3 h. ^b Neither of the dppp species given in ref. 28 showed any catalytic activity.

the formation of **22** by removal of CO, addition of PPh₃ or addition of PPh₃/H₂ proved unsuccessful.

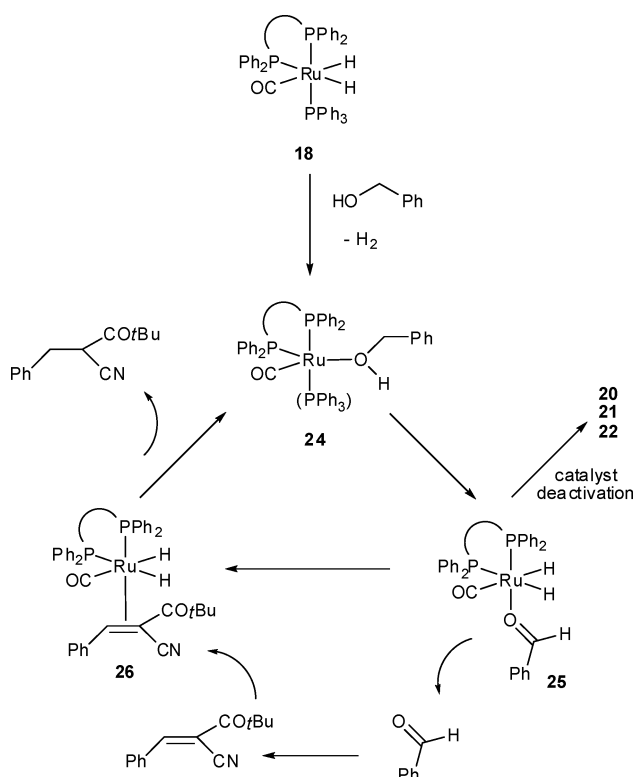
The ruthenium complexes **20–22** were tested for their activity in the benzylation of ketonitrile **6**, but all three were found to be less active than **18** (Table 4). Thus, although none of these three ruthenium complexes can therefore be associated with the overall catalytic Knoevenagel reaction, their formation reveals a relatively facile deactivation pathway that is available to **18**, at least under stoichiometric conditions.

Reactivity of **18** and **19** with benzaldehyde

The observation of free benzaldehyde and benzene upon reaction of **18** with benzyl alcohol prompted us to probe the reaction with benzaldehyde itself. In the presence of 5 equivalents of PhCHO (toluene, 120 °C, 1 h), **18** yielded a mixture of products. Both PhCH₂OH and benzene were observed in the proton NMR spectrum, while a ³¹P{¹H} spectrum showed a small amount of the ruthenium(0) species **21**, a significant amount of **22**, and small amounts of a new ruthenium containing complex **23** (Scheme 5). Complex **20** was not observed. ¹H and ¹³C NMR spectroscopy revealed that **23** contained a single hydride (δ -6.14 ppm, dd, ² $J_{\text{H-P}}$ = 121.3 Hz, ² $J_{\text{H-P}}$ = 25.8 Hz), one xantphos ligand and two carbonyl groups. The identity of the remaining sixth ligand could not be elucidated; an acyl group was excluded as no high frequency ¹³C resonance was detected, even when ¹³C labelling experiments were employed.³⁰ Efforts to isolate **23** from the reaction mixture or prepare it independently by either thermolysis or photolysis of **22** in the presence of PhCHO proved unsuccessful. Given the presence of the benzene in the reaction mixture, it seems plausible to suggest that **23** may correspond to the phenyl hydride complex [Ru(xantphos)(CO)₂(Ph)H] (Scheme 5, X = Ph), which would be



Scheme 5 Ruthenium products arising from reaction of [Ru(xantphos)-(PPh₃)(CO)H₂] (**18**) with benzaldehyde.



Scheme 6 Proposed reaction pathways of the xantphos complex **18** for catalytic Knoevenagel chemistry and stoichiometric decarbonylation.

formed following decarbonylation of the presumed acyl precursor [Ru(xantphos)(CO)(COPh)H].

While the dppp complex **19** also proved to be reactive towards 5 equivalents of PhCHO, a ³¹P{¹H} NMR spectrum of the reaction mixture revealed the formation of several low intensity Ru–phosphine containing products, along with a large amount of free PPh₃. While ¹H NMR showed signals for free PhCH₂OH, no major ruthenium hydride containing species could be detected.

Proposed mechanism for the catalyst action in the alkylation of **6**

In light of the information on the deactivation chemistry of **18**, a plausible mechanistic pathway for the Knoevenagel reaction of **1a** with **18** as the catalytic precursor is shown in Scheme 6. Under the reaction conditions of 120 °C, loss of hydrogen from **18** would be accessible,³¹ allowing the incoming benzyl alcohol to co-ordinate. Oxidative addition of the O–H bond followed by β-hydride elimination would afford benzaldehyde. While the benzaldehyde could act as a ligand (as shown for the putative intermediate complex **25**), the need for piperidinium acetate in the conversion of benzaldehyde and **6** into alkene suggests that this process may occur without any involvement of the ruthenium centre. The alkene could return to the ruthenium, where upon hydrogenation would generate the final organic product **7a** and regenerate a catalytically active ruthenium fragment. Under the stoichiometric conditions described above, in which the aldehyde would not be consumed by ketonitrile, loss of hydrogen from **25** could take place followed by oxidative addition into the C–H bond of the aldehyde, decarbonylation of the resulting aldehyde (to afford **23**), elimination of benzene and re-addition of H₂ to yield the dicarbonyl species **20**. The formation of the xantphos–PPh₃

complex **21** implies that there must also be a pathway involving the reversible dechelation of the xantphos ligand (this is needed to get to Ru(0) and retain the PPh₃ ligand); it may be that the dechelation process (which is assumed to be rapid)²⁰ accounts for the broadened NMR signals seen for **18**. The formation of the other ruthenium(0) complex **22** as the ultimate product of decarbonylation also requires the xantphos ligand to dechelate.

Conclusions

Xanthene based phosphine ligands have been shown to afford ruthenium dihydride complexes, which are catalytically active for the alkylation of alcohols by the ketonitrile **6**. The high reactivity of the xantphos complex [Ru(xantphos)(PPh₃)(CO)H₂] **18** contrasts with that of the dppp analogue **19**, which proves to be totally unreactive. While we cannot say precisely why the two ligands impart such different properties, that they do so is revealed very simply in the differing stoichiometric behaviour with PhCH₂OH. In the absence of **6**, **18** decarbonylates benzyl alcohol to afford [Ru(xantphos)(CO)₂H₂] and finally [Ru(xantphos)(CO)₃]. While the decarbonylation chemistry is not involved in the pathway for the Knoevenagel reaction, it provides us with a ‘marker’ for catalytic activity.

Experimental

General considerations

Manipulations were carried out using standard Schlenk or glovebox techniques under argon. Solvents were purified using either an Innovative Technologies solvent system (THF, hexane) or distilled under nitrogen from sodium benzophenone ketyl (toluene, benzene) or Mg–I₂ (EtOH). NMR spectra were recorded on Bruker Avance 300, 400 and 500 MHz NMR spectrometers, and referenced as follows: CDCl₃ (¹H, δ 7.27 ppm; ¹³C{¹H} δ 77.2 ppm), toluene (¹H, δ 2.09 ppm; ¹³C{¹H}, δ 21.3 ppm). ³¹P{¹H} NMR chemical shifts were referenced externally to 85% H₃PO₄ (δ 0.0 ppm). IR spectra were recorded on a Nicolet Nexus FTIR spectrometer. Mass spectrometry of organic products was performed by the EPSRC National Mass Spectrometry Service Centre, Swansea, UK, while mass spectra of the ruthenium complexes were recorded in the Department of Chemistry, University of Bath using a micrOTOF electrospray time-of-flight (ESI-TOF) mass spectrometer (Bruker Daltonik GmbH) coupled to an Agilent 1200 LC system (Agilent Technologies). Elemental analyses were performed by Elemental Microanalysis Ltd, Okehampton, Devon, UK. [Ru(PPh₃)₃(CO)H₂]³² and [Ru(dppp)(PPh₃)(CO)H₂]^{18a} were prepared according to literature procedures.

Representative catalytic procedure: 4,4-dimethyl-3-oxo-2-benzylpentanenitrile (7a). To a solution of benzyl alcohol **1a** (310 μL, 3 mmol) and 4,4-dimethyl-3-oxopentanenitrile **6** (376 mg, 3 mmol) in toluene (3.0 mL) in a carousel reaction tube was added [Ru(PPh₃)₃(CO)H₂] (13.9 mg, 0.015 mmol), xantphos **5** (8.6 mg, 0.015 mmol) and piperidinium acetate (21.8 mg, 0.15 mmol). The reaction mixture was heated to 110 °C in a pre-heated carousel reaction station and stirred for 3 h. After cooling, the solvent was removed *in vacuo* and the crude product was purified by column chromatography on silica using 19 : 1 petroleum ether (bp 40–60 °C)–ether as the eluent, giving the title compound

(509 mg, 79% isolated yield) as a colourless oil. Found: C 78.01, H 7.95, N 6.48. $C_{14}H_{17}NO$ requires C 78.10, H 7.41, N 6.06%. 1H NMR ($CDCl_3$, 300 MHz, 298 K) δ /ppm: 7.25–7.09 (m, 5H, ArH), 3.96 (app. t, $^3J_{HH} = 7.6$ Hz, 1H, –CH–), 3.11 (dd, $^2J_{HH} = 13.6$ Hz, $^3J_{HH} = 7.6$ Hz, 1H, –CHH–), 3.03 (dd, $^2J_{HH} = 13.6$ Hz, $^3J_{HH} = 7.6$ Hz, 1H, –CHH–), 0.99 (s, 9H, –C(CH₃)₃). $^{13}C\{^1H\}$ NMR ($CDCl_3$, 75.5 MHz, 298 K) δ /ppm: 205.2 (CO), 136.4 (ArC₁), 129.3 (ArC₃), 129.1 (ArC₂), 127.8 (ArC₄), 117.3 (–CN), 45.7 (–C(CH₃)₃), 38.9 (–CH–), 36.2 (–CH₂–), 25.8 (–C(CH₃)₃). IR (Nujol, ν/cm^{-1}): 2242 (s) $\nu(CN)$, 1716 (s) $\nu(CO)$. HRMS (ESI): $m/z = 233.1649$ (calcd 233.1648 for $[M - NH_4]^+$).

[Ru(xantphos)(PPh₃)(CO)H₂] (18). To a solution of $[Ru(PPh_3)_3(CO)H_2]$ (0.25 g, 0.27 mmol) in toluene (10 mL) was added xantphos (0.19 g, 0.33 mmol) and the mixture heated to 120 °C for 3 h. Removal of solvent gave a red oily residue, which was washed with EtOH (2 × 10 mL) and hexane (1 × 10 mL). The resulting solid was recrystallised from benzene–hexane to give **18** as an orange solid (0.121 g, 46% yield). Selected 1H NMR ($[d_8]$ -toluene, 500 MHz, 298 K) δ /ppm: –6.67 (dddd, $^2J_{HP} = 35.0$ Hz, $^2J_{HP} = 28.0$ Hz, $^2J_{HP} = 15.5$ Hz, $^2J_{HH} = 6.6$ Hz, 1H, RuH), –8.72 (ddd, $^2J_{HP} = 77.0$ Hz, $^2J_{HP} = 33.9$ Hz, $^2J_{HP} = 27.3$ Hz, $^2J_{HH} = 6.6$ Hz, 1H, RuH); $^{31}P\{^1H\}$ ($[d_8]$ -toluene, 202 MHz, 203 K) δ /ppm: 30.5 (br m), 45.2 (dd, $^2J_{PP} = 239.1$, $^2J_{PP} = 15.3$ Hz), 58.5 (dd, $^2J_{PP} = 237.2$ Hz, $^2J_{PP} = 15.5$ Hz). Selected $^{13}C\{^1H\}$ ($[d_8]$ -toluene, 125 MHz, 298 K) δ /ppm: 205.7 (m, CO). IR (KBr) ν/cm^{-1} : 1946 (s) $\nu(CO)$. Elemental analysis calcd (%) for $C_{58}H_{49}O_2P_3Ru$ (971.96): C 71.66, H 5.08; found: C 71.14, H 5.29; ESI-TOF MS: $[M + H - H_2]^+$ $m/z = 971.1917$ (theoretical 971.1921).

[Ru(xantphos)(CO)₃] (22). $[Ru_3(CO)_{12}]$ (0.1 g, 0.16 mmol) and xantphos (0.27 g, 0.47 mmol) were dissolved in toluene (20 mL) and the solution transferred to a 100 mL stainless-steel autoclave. The sample was placed under 25 atm CO and heated at 100 °C for 72 h. The solution was then cooled to room temperature, the pressure released and the yellow solution transferred to a Schlenk tube. Removal of the solvent afforded a yellow-orange oil, which was crystallized from benzene–hexane to give **22** as crystalline yellow blocks. (0.25 g, 70% yield). $^{31}P\{^1H\}$ ($[d_8]$ -toluene, 162 MHz, 298 K) δ /ppm: 27.9 (s). Selected $^{13}C\{^1H\}$ ($[d_8]$ -toluene, 100 MHz, 298 K) δ /ppm: 215.4 (t, $^2J_{CP} = 3.6$ Hz, CO). IR (Nujol) ν/cm^{-1} : $\nu(CO)$ 2007 (s), 1921 (s), 1920 (s). Elemental analysis calcd (%) for $C_{42}H_{32}O_4P_2Ru$ (763.70): C 66.05, H 4.22; found: C 66.11, H 4.28.

[Ru(xantphos)(CO)₂H₂] (20). A THF (10 mL) solution of **22** (0.05 g, 0.065 mmol) was photolysed (300 W Xe arc) at ca. 0 °C under a steady flow of H₂ for 0.5 h. In this time, the orange solution turned a pale straw colour. The solvent was removed under vacuum to leave a pale yellow residue, which was washed with EtOH (10 mL) and hexane (2 × 10 mL). The resulting solid was recrystallised from THF–EtOH to give **20** as small, pale yellow crystals (0.037 g, 76% yield). Selected 1H NMR ($[d_8]$ -toluene, 500 MHz, 298 K) δ /ppm: –6.13 (ddd, $^2J_{HP} = 26.8$ Hz, $^2J_{HP} = 17.6$ Hz, $^2J_{HH} = 6.5$ Hz, 1H, RuH), –7.65 (ddd, $^2J_{HP} = 83.1$ Hz, $^2J_{HP} = 30.5$ Hz, $^2J_{HH} = 6.5$ Hz, 1H, RuH). $^{31}P\{^1H\}$ ($[d_8]$ -toluene, 202 MHz, 298 K) δ /ppm: 24.6 (d, $^2J_{PP} = 21.5$ Hz), 35.1 (d, $^2J_{PP} = 21.5$ Hz). Selected $^{13}C\{^1H\}$ ($[d_8]$ -toluene, 125 MHz, 298 K) δ /ppm: 203.3 (dd, $^2J_{CP} = 81.9$ Hz, $^2J_{CP} = 7.1$ Hz, CO), 201.5 (dd, $^2J_{CP} = 11.2$ Hz, $^2J_{CP} = 8.5$ Hz, CO). IR (Nujol) ν/cm^{-1} : $\nu(CO)$ 2007 (s),

1960 (s). Elemental analysis calcd (%) for $C_{41}H_{34}O_3P_2Ru$ (737.71): C 66.75, H 4.65; found: C 66.66, H 4.63.

Acknowledgements

We thank the EPSRC for funding and Professor P. W. N. M. van Leeuwen for the gift of ligands **12–15**.

Notes and references

- G. Zassinovich, G. Mestroni and S. Gladiali, *Chem. Rev.*, 1992, **92**, 1051; M. J. Palmer and M. Wills, *Tetrahedron: Asymmetry*, 1999, **10**, 2045; S. Gladiali and E. Alberico, *Chem. Soc. Rev.*, 2006, **35**, 226.
- R. Grigg, T. R. B. Mitchell, S. Sutthivaiyakit and N. Tongpenyai, *Tetrahedron Lett.*, 1981, **22**, 4107.
- For reviews of C–C bond formation from alcohols by borrowing hydrogen see: G. Guillena, D. J. Ramón and M. Yus, *Angew. Chem., Int. Ed.*, 2007, **46**, 2358; M. H. S. A. Hamid, P. A. Slatford and J. M. J. Williams, *Adv. Synth. Catal.*, 2007, **349**, 1555.
- Examples of Ru catalysts: C. S. Cho, B. T. Kim, T.-J. Kim and S. C. Shim, *J. Org. Chem.*, 2001, **66**, 9020; K. Motokura, D. Nishimura, K. Mori, T. Mizugaki, K. Ebitani and K. Kaneda, *J. Am. Chem. Soc.*, 2004, **126**, 5662; R. Martinez, G. J. Brand, D. J. Ramón and M. Yus, *Tetrahedron Lett.*, 2005, **46**, 3683.
- Examples of Ir catalysts: K. Fujita and R. Yamaguchi, *Synlett*, 2005, 560; C. Löfberg, R. Grigg, A. Keep, A. Derrick, V. Sridharan and C. Kilner, *Chem. Commun.*, 2006, 5000; C. Löfberg, R. Grigg, M. A. Whittaker, A. Keep and A. Derrick, *J. Org. Chem.*, 2006, **71**, 8023; M. Morita, Y. Obara and Y. Ishii, *Chem. Commun.*, 2007, 2850.
- Examples of Pd catalysts: C. S. Cho, *J. Mol. Catal. A: Chem.*, 2005, **240**, 55; M. S. Kwon, N. Kim, S. H. Seo, I. S. Park, R. K. Cheedra and J. Park, *Angew. Chem., Int. Ed.*, 2005, **44**, 6913; Y. M. A. Yamada and Y. Uozumi, *Org. Lett.*, 2006, **8**, 1375.
- M. G. Edwards and J. M. J. Williams, *Angew. Chem., Int. Ed.*, 2002, **41**, 4740.
- M. G. Edwards, R. F. R. Jazsar, B. M. Paine, D. J. Shermer, M. K. Whittlesey, J. M. J. Williams and D. D. Edney, *Chem. Commun.*, 2004, 90; see also: S. Burling, B. M. Paine, D. Nama, V. S. Brown, M. F. Mahon, T. J. Prior, P. S. Pregosin, M. K. Whittlesey and J. M. J. Williams, *J. Am. Chem. Soc.*, 2007, **129**, 1987.
- P. A. Slatford, M. K. Whittlesey and J. M. J. Williams, *Tetrahedron Lett.*, 2006, **47**, 6787; P. J. Black, G. Cami-Kobeci, M. G. Edwards, P. A. Slatford, M. K. Whittlesey and J. M. J. Williams, *Org. Biomol. Chem.*, 2006, **4**, 116.
- S. J. Pridmore, P. A. Slatford and J. M. J. Williams, *Tetrahedron Lett.*, 2007, **48**, 5111.
- S. J. Pridmore, P. A. Slatford, A. Daniel, M. K. Whittlesey and J. M. J. Williams, *Tetrahedron Lett.*, 2007, **48**, 5115.
- N. Anand, N. A. Owston, A. J. Parker, P. A. Slatford and J. M. J. Williams, *Tetrahedron Lett.*, 2007, **48**, 7761.
- A. R. Elmaghrabi, G. Gassner, H. Gorgs and E. Dinjus, *J. Organomet. Chem.*, 2000, **597**, 139.
- P. C. J. Kamer, P. W. N. M. van Leeuwen and J. N. H. Reek, *Acc. Chem. Res.*, 2001, **34**, 895; Z. Freixa and P. W. N. M. van Leeuwen, *Dalton Trans.*, 2003, 1890.
- G. Dube, D. Selent and R. Taube, *Z. Angew. Chem.*, 1985, **25**, 154.
- P. Dierkes and P. W. N. M. van Leeuwen, *J. Chem. Soc., Dalton Trans.*, 1999, 1519; P. W. N. M. van Leeuwen, P. C. J. Kamer, J. N. H. Reek and P. Dierkes, *Chem. Rev.*, 2000, **100**, 2741.
- L. A. van der Veen, P. K. Keeven, G. C. Schoemaker, J. N. H. Reek, P. C. J. Kamer, P. W. N. M. van Leeuwen, M. Lutz and A. L. Spek, *Organometallics*, 2000, **19**, 872; J. J. Carbó, F. Maseras, C. Bo and P. W. N. M. van Leeuwen, *J. Am. Chem. Soc.*, 2001, **123**, 7630.
- C. W. Jung and P. E. Garrou, *Organometallics*, 1982, **2**, 658; H. Kawano, R. Tanaka, T. Fujikawa, K. Hiraki and M. Onishi, *Chem. Lett.*, 1999, 401.
- Jung and Garrou reported for a variety of different P–P that the PPh₃ resonance in $[Ru(P-P)(PPh_3)(CO)H_2]$ appears at δ ca. 59 ppm in the $^{31}P\{^1H\}$ NMR spectrum (ref. 18a). The ^{31}P signals in **18** are assigned on this basis.
- Heating **18** with 3 equiv. of P(*p*-tolyl)₃ at 70 °C for 15 h failed to show any evidence for phosphine exchange or coordination.

- 21 M. A. Zuideveld, B. H. G. Swennenhuis, M. D. K. Boele, Y. Guari, G. P. F. van Strijdonck, J. N. H. Reek, P. C. J. Kamer, K. Goubitz, J. Fraanje, M. Lutz, A. L. Spek and P. W. N. M. van Leeuwen, *J. Chem. Soc., Dalton Trans.*, 2002, 2308; K. A. Leñero, M. Kranenburg, Y. Guari, P. C. J. Kamer, P. W. N. M. van Leeuwen, S. Sabo-Etienne and B. Chaudret, *Inorg. Chem.*, 2003, **42**, 2859.
- 22 P. H. M. Budzelaar, *g-NMR, version 4*, Cherwell Scientific Publishing Ltd., Oxford, UK, 1995–1997.
- 23 Crystal Data for **18**, $C_{55}H_{49}O_2P_3Ru$, $M = 971.95$, $T = 150$ K, $\lambda = 0.71073$ Å, triclinic, space group $P\bar{1}$ (no. 2), $a = 11.0940(1)$, $b = 12.9620(1)$, $c = 18.1840(2)$ Å, $\alpha = 92.599(1)$, $\beta = 92.909(1)$, $\gamma = 113.854(1)^\circ$, $U = 2382.20(4)$ Å³, $Z = 2$, $D_c = 1.355$ g cm⁻³, $\mu = 0.473$ mm⁻¹, $F(000) = 1004$, crystal size $0.20 \times 0.12 \times 0.07$ mm, unique reflections = 10 813 [$R_{int} = 0.0523$], observed $I > 2\sigma I = 9114$, data/restraints/parameters = 10 813/0/632, $R_1 = 0.0399$ w $R_2 = 0.07$ (observed data), $R_1 = 0.0549$ w $R_2 = 0.080$ (all data), max. peak/hole 0.466 and -0.579 e Å⁻³, software used, SHELXS, SHELXL and ORTEX. Hydrides, located and refined at 1.6 Å from Ru1. 50 : 50 disorder in phenyl carbons C36–C40.
- 24 This compound was identified by an independent synthesis using the method of Duckett and co-workers (D. Blazina, J. P. Dunne, S. Aiken, S. B. Duckett, C. Elkington, J. E. McGrady, R. Poli, S. J. Walton, M. S. Anwar, J. A. Jones and H. E. Carteret, *Dalton Trans.*, 2006, 2072) by heating $[Ru(PPh_3)_2(CO)_3]$ with xantphos. $^{31}P\{^1H\}$ ($[d_8]$ -toluene, 298 K) δ /ppm: 34.4 (d, $^2J(P,P) = 84.3$ Hz), 54.8 (d, $^2J(P,P) = 84.3$ Hz); IR (Nujol) ν/cm^{-1} : $\nu(CO)$ 1909 (s), 2003 (s). ESI-TOF MS: $[M + H - CO]^+ m/z = 971.1990$ (theoretical 971.1990).
- 25 A small amount of a second species, which displayed a doublet hydride resonance at $\delta -7.63$ ppm [$^2J(H,P) = 45.7$ Hz] and a singlet ^{31}P resonance at $\delta 29.2$ ppm, was always detected in the formation of **20**, but efforts to either generate this complex in higher yield or separate it were unsuccessful.
- 26 M. K. Whittlesey, R. N. Perutz, I. G. Virrels and M. W. George, *Organometallics*, 1996, **16**, 268; T. Gottschalk-Gaudig, K. Foltling and K. G. Caulton, *Inorg. Chem.*, 1999, **38**, 5241; D. Schott, C. J. Sleigh, J. P. Lowe, S. B. Duckett, R. J. Mawby and M. G. Partridge, *Inorg. Chem.*, 2002, **41**, 2960; D. Schott, P. Callaghan, J. P. Dunne, S. B. Duckett, C. Godard, J. M. Goicoechea, J. N. Harvey, J. P. Lowe, R. J. Mawby, G. Müller, R. N. Perutz, R. Poli and M. K. Whittlesey, *Dalton Trans.*, 2004, 3218.
- 27 The X-ray crystal structure† of **22** is reported in the ESI.
- 28 The dppp complexes, $[Ru(dppp)(CO)_2H_2]$ and $[Ru(dppp)(CO)_3]$, were prepared *via* analogous procedures to those used for **20** and **22**.
- 29 Crystal Data for **20**, $C_{41}H_{34}O_3P_2Ru$, $M = 737.69$, $T = 150$ K, $\lambda = 0.71073$ Å, triclinic, space group $P\bar{1}$ (no. 2), $a = 10.0620(2)$, $b = 10.6710(2)$, $c = 18.1510(4)$ Å, $\alpha = 73.413(1)$, $\beta = 73.881(1)$, $\gamma = 73.441(1)^\circ$, $U = 1749.00(6)$ Å³, $Z = 2$, $D_c = 1.401$ g cm⁻³, $\mu = 0.577$ mm⁻¹, $F(000) = 756$, crystal size $0.08 \times 0.08 \times 0.06$ mm, unique reflections = 7924 [$R_{int} = 0.0703$], observed $I > 2\sigma I = 5643$, data/restraints/parameters = 7924/2/435, $R_1 = 0.0478$ w $R_2 = 0.0800$ (observed data), $R_1 = 0.0841$ w $R_2 = 0.0909$ (all data), max. peak/hole 0.510 and -1.125 e Å⁻³, software used, SHELXS, SHELXL and ORTEX. Hydrides, located and refined at 1.6 Å from Ru1.
- 30 M. P. Waugh, R. J. Mawby, A. J. Reid, R. J. Carter and C. D. Reynolds, *Inorg. Chim. Acta*, 1995, **240**, 263.
- 31 H–D exchange between the hydride ligands of **18** and D₂ (1 atm) was apparent by 1H NMR spectroscopy after just 30 min at 50 °C.
- 32 N. Ahmad, J. J. Levison, S. D. Robinson and M. F. Uttley, *Inorg. Synth.*, 1974, **15**, 48.